Optics Letters

Microwave channelizer based on a photonic dual-output image-reject mixer

Wenjuan Chen,[1] Dan Zhu,[1,2] Chenxu Xie,[1] Jiang Liu,[1] and Shilong Pan[1,3]

[1]Key laboratory of Radar Imaging and Microwave Photonics, Ministry of Education, Nanjing University of Aeronautics and Astronautics, Nanjing 210016, China
[2]e-mail: danzhu@nuaa.edu.cn
[3]e-mail: pans@nuaa.edu.cn

Received 6 May 2019; revised 14 July 2019; accepted 15 July 2019; posted 22 July 2019 (Doc. ID 366799); published 13 August 2019

A microwave channelizer based on a photonic dual-output image-reject mixer (IRM) is proposed and demonstrated. By introducing the dual-output IRM based on the balanced Hartley structure, 2*N* channels can be produced by using the optical frequency combs (OFCs) with *N* comb lines. The required electrical hybrids and the optical filters are also reduced by half. In addition, the channelization efficiency is doubled, and the in-band interferences, including the image and the nonlinear mixing spurs, are greatly suppressed. A proof-of-concept experiment is performed. By applying a pair of OFCs with three comb lines, an RF signal with a 6 GHz instantaneous bandwidth is successfully divided into six channels with 1 GHz bandwidth. The in-band interference is suppressed by more than 25 dB for all channels.

https://doi.org/10.1364/OL.44.004052

RF signal channelization has been widely studied in recent years due to its wideband RF signal processing capability, which is highly required in modern RF systems, including radar [1], electronic warfare [2], communication system [3], and satellite payload [4]. Through the RF signal channelization, a broadband RF signal will be sliced into a number of narrowband channels which can be directly processed by the state of the art electronics [5]. With the rapid increasing of the frequency and bandwidth in RF systems, microwave photonic channelization has attracted great attention due to the benefits introduced by photonics, including large bandwidth, parallel processing capability, and low transmission loss [6]. Three main methods are proposed to realize the microwave photonic channelization [7–15]. The first one is to convert the RF signal into the optical domain, which is then split into several consecutive channels by using optical filter arrays [7]. The second one is to copy the RF signal to a group of optical carriers (typically an optical frequency comb [OFC]), which are then filtered by a periodic optical filter with a slightly different comb line spacing to select different components of the RF signal [8–13]. For the above two methods, however, strict requirements of the optical filters in terms of precise center frequency, narrow bandwidth, flat top, steep edge, and so on must be satisfied in order to guarantee the channelization quality.

The third method to implement the microwave photonic channelization is coherent channelization based on two OFCs [14,15]. One OFC is used to broadcast the RF signal, and the other one with a slightly different comb line spacing is used to downconvert different components of the RF signal, which are sliced into different channels using a multichannel optical filter with low requirements. The two OFCs can also be replaced by two linearly frequency-modulated (LFM) optical pulses with proper time delay [16]. The LFM optical source plays as an OFC with comb lines sweeping with time. The frequency difference between the two OFCs is realized through the introduced time delay. However, for all these approaches, only one channel can be output from each copy of the RF signal in the optical domain for each photonic LO. The channelization efficiency is low. In addition, the comb line number of the OFCs must be equal to the channel number, demanding coherent OFCs with high quality and large comb lines which are difficult to generate, especially when the number of the channelization channels is large.

In this Letter, a microwave channelizer is proposed and demonstrated based on the photonic dual-output image-reject mixer (IRM). Making use of the microwave photonic dual-output IRM based on the balanced Hartley structure, two sub-channels will be generated from each copy of the RF signal in the optical domain with one photonic LO. The required OFC comb line number is reduced by half, and the channelization efficiency is doubled. As compared with Ref. [15], to realize a channelization with the same channel numbers, the required OFC comb line number, the electrical hybrids, and the OBPFs are reduced by half. In addition, by introducing the microwave photonic dual-output IRM based on a balanced Hartley structure, the in-band interference, including the image and the undesired mixing spurs can be suppressed simultaneously. In this way, the channel crosstalk suppression can be guaranteed. A proof of concept experiment is taken. By using OFCs with three comb lines, a Ku-band RF signal with a bandwidth of 6 GHz is successfully divided into six channels with a 1 GHz bandwidth. The in-band interference is suppressed by more 25 dB for all the channels.

The schematic diagram of the proposed microwave channelizer using the photonic dual-output IRM is shown in Fig. 1(a). A pair of OFCs (the signal OFC and the local OFC) with N comb lines is employed, the comb line spacing of which are f_S and $f_S + \Delta f$, respectively, as illustrated in Figs. 1(b) and 1(c). The frequencies of the nth comb line of the signal OFC and the local OFC can be expressed as $f_{\mathrm{Si\_OFC}}(n) = f_{\mathrm{Sig}}(1) + (n-1)f_S$, $f_{\mathrm{LO\_OFC}}(n) = f_{\mathrm{Sig}}(1) + f_0 + (n-1)(f_S + \Delta f)$, respectively, where $f_{\mathrm{Sig}}(1)$ is the frequency of the first comb line of the signal OFC, and f_0 is the frequency difference between the first comb lines of the two OFCs. The signal OFC is modulated by the RF signal $f_{\mathrm{RF}}(t)$ with the carrier-suppressed single-sideband (CS-SSB) modulation format, as shown in Fig. 1(b). The expression of the nth copy of the RF signal in the optical domain is $f_{\mathrm{si\_mod}}(n) = f_{\mathrm{Si\_OFC}}(n) + f_{\mathrm{RF}}(t) = f_{\mathrm{Si\_OFC}}(n) + f_{\mathrm{RL}n}(t) + f_{\mathrm{RR}n}(t)$, where $f_{\mathrm{RL}n}(t)$ and $f_{\mathrm{RR}n}(t)$ denote the frequency components of the optically carried RF signal located at the left and the right sides of the nth photonic LO $E_{\mathrm{LO}\_n}(t)$, respectively, as shown in Fig. 1(b). The modulated signal OFC and the LO OFC are selected by the photonic programmable processors and injected into the signal port and the LO port of a 90° optical hybrid, respectively, with the optical field expression as

$$\begin{cases} E_{\mathrm{Si}\_n}(t) \propto e^{\mathrm{j}2\pi t f_{\mathrm{Si\_mod}}(n)} = \underbrace{e^{j2\pi t[f_{\mathrm{Si\_OFC}}(n)+f_{\mathrm{RL}n}(t)]}}_{\text{while } f_{\mathrm{Si\_mod}}(n)<f_{\mathrm{LO\_OFC}}(n)} + \underbrace{e^{j2\pi t[f_{\mathrm{Si\_OFC}}(n)+f_{\mathrm{RR}n}(t)]}}_{\text{while } f_{\mathrm{Si\_mod}}(n)>f_{\mathrm{LO\_OFC}}(n)}. \\ E_{\mathrm{LO}\_n}(t) \propto e^{\mathrm{j}2\pi t f_{\mathrm{LO\_OFC}}(n)} \end{cases} \quad (1)$$

At the outputs of the 90° optical hybrid, two in-phase outputs ($I_1 \propto E_{\mathrm{Si}\_n} + E_{\mathrm{LO}\_n}$, $I_2 \propto E_{\mathrm{Si}\_n} - E_{\mathrm{LO}\_n}$) and two quadrature outputs ($Q_1 \propto E_{\mathrm{Si}\_n} + jE_{\mathrm{LO}\_n}$, $Q_2 \propto E_{\mathrm{Si}\_n} - jE_{\mathrm{LO}\_n}$) are injected into two balanced photodetectors (BPDs), respectively. A pair of quadrature downconverted IF signals will be obtained with the expressions as follows:

$$\begin{cases} i_{\mathrm{I}}(t) \propto \cos\{2\pi[f_{\mathrm{LO}}(n) - f_{\mathrm{RL}n}(t)]t\} + \cos\{2\pi[f_{\mathrm{RR}n}(t) - f_{\mathrm{LO}}(n)]t\} \\ i_{\mathrm{Q}}(t) \propto -\sin\{2\pi[f_{\mathrm{LO}}(n) - f_{\mathrm{RL}n}(t)]t\} + \sin\{2\pi[f_{\mathrm{RR}n}(t) - f_{\mathrm{LO}}(n)]t\} \end{cases}, \quad (2)$$

where $f_{\mathrm{LO}}(n) = f_{\mathrm{Si\_OFC}}(n) - f_{\mathrm{LO\_OFC}}(n) = f_0 + (n-1)\Delta f$. As can be seen from Eq. (2), the mixing spur at $f_{\mathrm{RR}n}(t) - f_{\mathrm{RL}n}(t)$ is eliminated. An electrical quadrature hybrid is used to combine the outputs of the two BPDs in Eq. (2). The structure of the electrical quadrature hybrid in detail is shown in the inset of Fig. 1(a), with the transform matrix as follows [17]:

$$[S] = \begin{bmatrix} S_{11} & S_{12} & S_{13} & S_{14} \\ S_{21} & S_{22} & S_{23} & S_{24} \\ S_{31} & S_{32} & S_{33} & S_{34} \\ S_{41} & S_{42} & S_{43} & S_{44} \end{bmatrix} = \frac{-1}{\sqrt{2}} \begin{bmatrix} 0 & j & 1 & 0 \\ j & 0 & 0 & 1 \\ 1 & 0 & 0 & j \\ 0 & 1 & j & 0 \end{bmatrix}. \quad (3)$$

Thus, the two outputs of the electrical quadrature hybrid can be expressed as

$$\begin{bmatrix} i_2 \\ i_3 \end{bmatrix} = \begin{bmatrix} S_{21} & S_{24} \\ S_{31} & S_{34} \end{bmatrix} \begin{bmatrix} i_{\mathrm{I}}(t) \\ i_{\mathrm{Q}}(t) \end{bmatrix} = \begin{bmatrix} -2\sin\{2\pi[f_{\mathrm{LO}}(n) - f_{\mathrm{RL}n}(t)]t\} \\ 2\cos\{2\pi[f_{\mathrm{RR}n}(t) - f_{\mathrm{LO}}(n)]t\} \end{bmatrix}. \quad (4)$$

As can be seen, the optically carried RF frequency components located at the left ($f_{\mathrm{RL}n}$) and right ($f_{\mathrm{RR}n}$) sides of the nth photonic LO are downconverted with the same equivalent LO of $f_{\mathrm{LO}}(n)$ and output from the two output ports of the electrical quadrature hybrid, respectively. The frequency components located at the left and right sides of the photonic LO are the image for each other. Thus, it can be seen that the microwave photonic dual-output image-reject mixing based on the balanced Hartley structure [18] is realized. The suppression of the downconverted image and the nonlinear mixing spurs are realized simultaneously, guaranteeing the channelization with low crosstalk. By introducing electrical bandpass filters centered at f_{IF} with a bandwidth of Δf to the two outputs, two different channelized components corresponding to Ch-n and Ch-$(n+N)$ with in-band crosstalk greatly suppressed will be achieved with the nth photonic LO $f_{\mathrm{LO\_OFC}}(n)$ and the nth copy of the RF signal in the optical domain $f_{\mathrm{Si\_mod}}(n)$, as shown in Fig. 1(d). In this way, the different parts of the received wideband RF signal will be downconverted to the same IF band with the center frequency of f_{IF} and the bandwidth of Δf, and $2N$ channels will be produced by using the OFCs with N comb lines. The optical LOs are reduced by half, and the channelization efficiency is improved, as compared with the former schemes [14–16].

An experiment utilizing the scheme shown in Fig. 1 is established, and the experimental setup is given in Fig. 2. A laser diode (LD, TeraXion NLL04) is used to generate an optical carrier with the wavelength of 1550.52 nm. The Lightwave is then divided into two parts. One part is injected into a Mach-Zehnder modulator (MZM1) driven by a single-tone RF signal of f_S to generate the signal OFC. The other part is first frequency shifted by f_{Shift} through an optical frequency shifter, which is composed of MZM2 driven by a single-tone RF signal of f_{Shift} and an optical bandpass filter (Yenista XTM-50) to select the shifted optical carrier. The frequency shifted

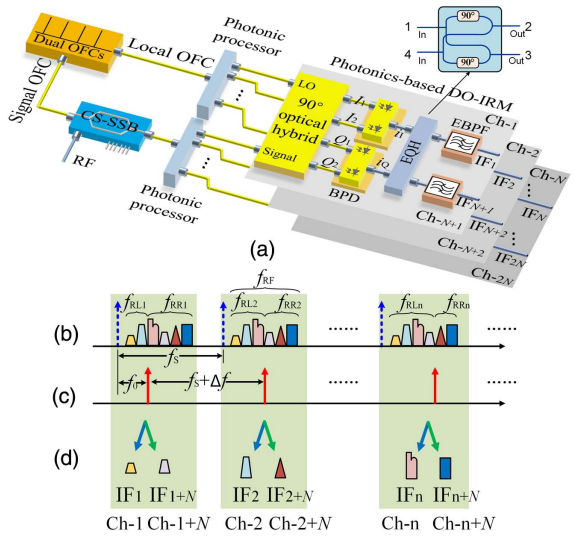

Fig. 1. (a) Schematic diagram of the proposed microwave channelizer based on the photonic dual-output IRM. (Inset: the principle structure of the electrical quadrature hybrid [EQH]). Illustrations of the optical spectra of (b) the signal OFC before and after modulation, (c) the local OFC, and (d) the electrical output of each channel. DPMZM, dual-parallel Mach-Zehnder modulator; BPD, balanced photodetector; EQH, electrical quadrature hybrid; EBPF, electrical bandpass filter; IRM, image-reject mixer.

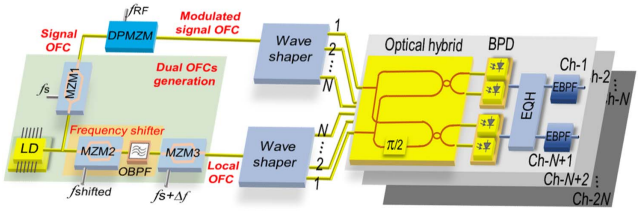

Fig. 2. Experimental setup of the proposed microwave photonic channelizer based on the dual-output IRM. LD, laser diode; MZM, Mach–Zehnder modulator; OBPF, optical bandpass filter; DPMZM, dual-parallel Mach-Zehnder modulator; BPD, balanced photodetector; EQH, electrical quadrature hybrid; EBPF, electrical bandpass filter.

optical carrier is injected into MZM3 driven by a single-tone signal of $f_S + \Delta f$ to generate the local OFC. The MZMs (Fujitsu FTM7938EZ) have a working frequency of 40 GHz. A dual-parallel Mach-Zehnder modulator (DPMZM, Fujitsu FTM7961EX) with a 3 dB bandwidth of 25 GHz is employed to multicast the RF signal to the signal OFC. An arbitrary waveform generator (AWG, Keysight 8195A, 65 GSa/s) is used to generate the RF signal. Two waveshapers (Finisar 16000s and 4000s) are served as photonic programmable processors. The BPDs (Finisar BPDV2150R) have the working bandwidth of 40 GHz and the responsivity of 0.53 A/W. The electrical quadrature hybrid (Pulsar QS8-13-463/7S) has the working frequency range of 0.5–10 GHz. The optical spectra are observed by the optical spectrum analyzer (OSA, YOKOGAWA AQ6370C) with the resolution of 0.02 nm. The electrical spectra are measured by the signal analyzer (R&S FSV-40, 10 Hz-40 GHz). In addition, an oscilloscope (Keysight Infiniium DSOX93304, 80 GSa/s) is used to observe the waveforms.

The comb line spacing of the signal OFC is set to be 26 GHz, and that of the local OFC is set to be 27 GHz. The frequency shift f_{shift} is set to be 10 GHz, making the value of f_0 (the frequency difference between the first comb lines of the two OFCs) be 9 GHz. The optical spectra of the obtained two OFCs are shown in Fig. 3. First, the performance of the microwave photonic dual-output IRM is experimentally investigated. The first comb lines of the two OFCs with frequency difference of 9 GHz are used. Two LFM RF signals with the same 1 GHz bandwidth centered at 7.5 and 10.5 GHz are modulated at the selected signal OFC comb line 1, respectively. The two optically carried RF signals are located at the left and right sides of the selected photonic LO comb line 1 in the frequency domain. When the RF signal centered at 7.5 GHz is

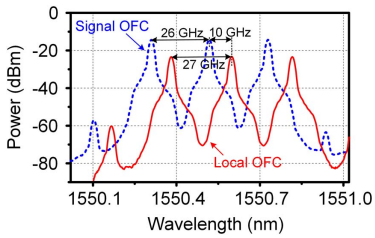

Fig. 3. Experimentally obtained optical spectra of the signal OFC (blue dotted line) and the local OFC (red solid line).

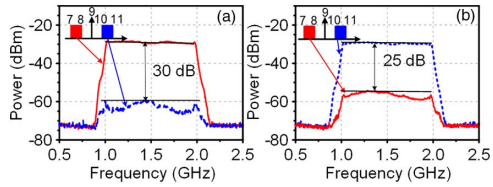

Fig. 4. Measured electrical spectra of the output signals at the output (a) port 1 and (b) port 2 of the electrical quadrature hybrid when the RF signals with the same 1 GHz bandwidth centered at 7.5 GHz (red solid line) and 10.5 GHz (blue dashed line) are applied.

applied, the two outputs of the electrical quadrature hybrid are shown as the red solid lines in Figs. 4(a) and 4(b), respectively. By applying the RF signal centered at 10.5 GHz, the two outputs of the electrical quadrature hybrid are shown as the blue dashed line, respectively. It can be seen that the two optically carried RF signals located at the left and right sides of the photonic LO are downconverted to the same IF band and output from the two output ports of the same electrical quadrature hybrid, respectively. In this way, a dual-output IRM using the balanced Hartley structure is realized. As can be seen, the image rejection ratio is higher than 25 dB within 1 GHz bandwidth. The image rejection ratio difference for the two output ports is due to the phase and amplitude imbalances of the used electrical quadrature hybrid.

Then the channelization is realized based on the dual-output IRM. A wideband LFM RF signal covering 7–13 GHz with 1 μs time duration is modulated at the signal OFC with the CS-SSB modulation format. Figure 5 shows the optical spectra of the modulated signal OFC and the LO OFC. The photonic programmable processors are used to select the corresponding photonic LOs and the optically carried RF signals, as shown in Fig. 5. By introducing the microwave photonic dual-output image-reject mixing, two channels will be output for each photonic LO, and each copy of the RF signal in the optical domain. Figure 6 shows the output electrical spectra of the downconverted IF signals before and after electrical filtering in each channel. The insets illustrate the locations of the RF copy in the optical domain and the corresponding photonic LO. The two downconverted IF components corresponding to photonic LO1 are shown as the blue dashed lines in Figs. 6(a1) and 6(a2), with the frequency range of 0–2 and 0–4 GHz, respectively. It can be seen that the optically carried RF components located at the left and right sides of photonic LO1 are downconverted and output simultaneously, with the bandwidth of 2 and 4 GHz, respectively. The out-of-band crosstalk rejection

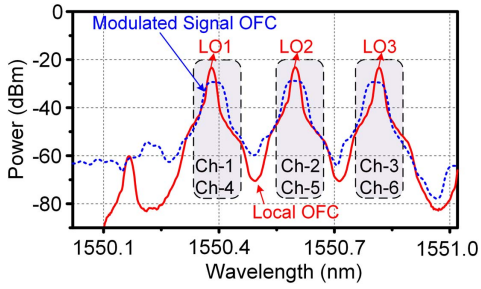

Fig. 5. Measured optical spectra of the modulated signal OFC (blue dotted line) and the local OFC (red solid line).

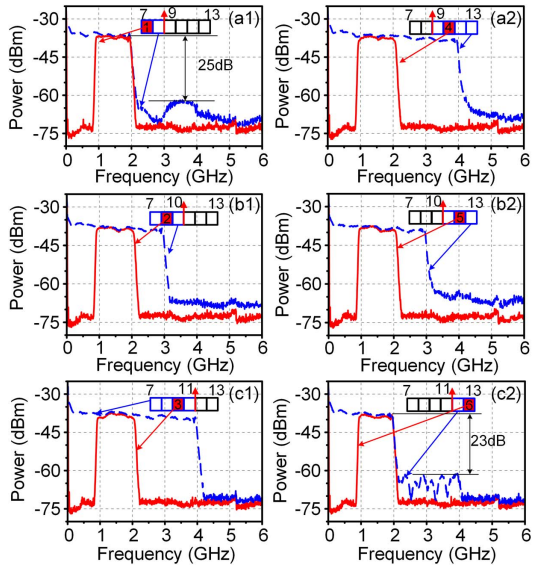

Fig. 6. Output electrical spectra of the downconverted IF signals before (blue dashed line) and after (red solid line) electrical filtering for (a1)–(c1) Ch-1 to Ch-3 and (a2)–(c2) Ch-4 to Ch-6.

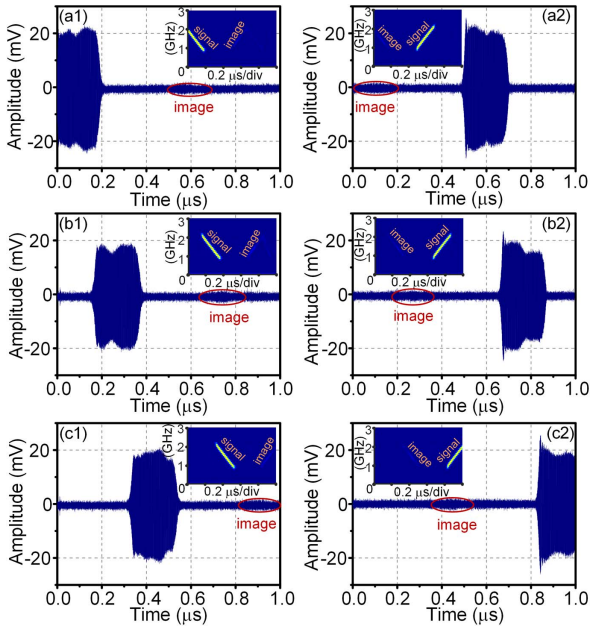

Fig. 7. Output 1–2 GHz IF signal waveforms at the (a1)-(c1) Ch-1 to Ch-3 and (a2)-(c2) Ch-4 to Ch-6. Inset: the corresponding instantaneous frequency-time diagram.

ratio is large than 25 dB. By applying the EBPFs with the center frequency of 1.5 GHz and the bandwidth of 1 GHz at each output port of the electrical quadrature hybrid, channel 1 and channel 4 are realized. The corresponding IF components in channels 1 and 4 are downconverted from the 7–8 and 10–11 GHz RF components, as shown as the red solid lines in Figs. 6(a1) and 6(a2), respectively. The out-of-band crosstalk is further suppressed to be more than 35 dB. Similarly, with photonic LO2, channels 2 and 5 downconverted from 8–9 and 11–12 GHz RF components are obtained, with the results shown in Figs. 6(b1) and 6(b2). The 9–10 and 12–13 GHz RF components are downconverted with photonic LO3, forming the channels 3 and 6, with the results shown in Figs. 6(c1) and 6(c2), respectively.

The corresponding waveforms of the channelized output IF signals at 1–2 GHz in each channel are shown in Fig. 7, and the inserts are the corresponding instantaneous frequency-time diagrams. It can be seen that the crosstalk has been greatly suppressed for each channel. In this way, the RF signal with a 6 GHz bandwidth centered at 10 GHz is successfully channelized to six channels by using OFCs with only three comb lines.

In conclusion, we have proposed and demonstrated a photonic microwave channelizer with greatly reduced requirement of the comb line number of the OFCs. With a photonic dual-output IRM based on the balanced Hartley structure, $2N$ channels can be produced by using the OFCs with N comb lines. In-band interference can also be greatly suppressed because of the IRM. The proposed scheme can find applications in RF systems with high operational frequency and a large instantaneous bandwidth for radars, communications, and electrical warfare.

Funding. Natural Science Foundation of Jiangsu Province (BK20160082); Jiangsu Provincial Program for High-level Talents in Six Areas (DZXX-030); Jiangsu Province "333" project (BRA2018042); Fundamental Research Funds for the Central Universities (NC2018005, NE2017002).

REFERENCES

1. F. Z. Zhang, Q. S. Guo, Z. Q. Wang, P. Zhou, G. Q. Zhang, J. Sun, and S. L. Pan, Opt. Express **25**, 16274 (2017).
2. G. W. Anderson, D. C. Webb, A. E. Spezio, and J. N. Lee, Proc. IEEE **79**, 355 (1991).
3. X. Zou, W. Bai, W. Chen, P. Li, B. Lu, G. Yu, W. Pan, B. Luo, L. Yan, and L. Shao, J. Lightwave Technol. **36**, 4337 (2018).
4. S. L. Pan, D. Zhu, S. F. Liu, K. Xu, Y. T. Dai, T. L. Wang, J. G. Liu, N. H. Zhu, Y. Xue, and N. J. Liu, IEEE Microw. Mag. **16**, 61 (2015).
5. W. Namgoong, IEEE Trans. Wireless Commun. **2**, 502 (2003).
6. J. P. Yao, J. Lightwave Technol. **27**, 314 (2009).
7. D. B. Hunter, L. G. Edvell, and M. A. Englund, in *IEEE International Topical Meeting on Microwave Photonics* (2005), p. 249.
8. X. W. Gu, D. Zhu, S. M. Li, Y. J. Zhao, and S. L. Pan, in *7th IEEE/International Conference on Advanced Infocomm Technology (ICAIT)* (2014), p. 240.
9. X. Xie, Y. Dai, Y. Ji, K. Xu, Y. Li, J. Wu, and J. Lin, IEEE Photonics Technol. Lett. **24**, 661 (2012).
10. X. Zou, W. Pan, B. Luo, and L. Yan, Opt. Lett. **35**, 438 (2010).
11. Z. Li, H. Chi, X. M. Zhang, S. L. Zheng, X. F. Jin, and J. P. Yao, in *IEEE International Topical Meeting on Microwave Photonics, Asia-Pacific Microwave Photonics Conference* (2011), p. 296.
12. W. Y. Xu, D. Zhu, and S. L. Pan, Opt. Eng. **55**, 046106 (2016).
13. H. Huang, C. Zhang, H. Zhou, H. Yang, W. Yuan, and K. Qiu, Opt. Lett. **43**, 4073 (2018).
14. X. Xie, Y. Dai, K. Xu, J. Niu, R. Wang, L. Yan, and J. Lin, IEEE Photonics J. **4**, 1196 (2012).
15. Z. Z. Tang, D. Zhu, and S. L. Pan, J. Lightwave Technol. **36**, 4219 (2018).
16. W. Hao, Y. Dai, F. Yin, Y. Zhou, J. Li, J. Dai, W. Li, and K. Xu, Opt. Lett. **42**, 5234 (2017).
17. D. M. Pozar, *Microwave Engineering*, 3rd ed. (Wiley, 2005), Chap. 7.
18. D. Zhu, W. J. Chen, and S. L. Pan, Opt. Express **26**, 28022 (2018).